BMC Cancer

RESEARCH Open Access

Tumor suppressing function of *SLC16A7* in bladder cancer and its pan-cancer analysis

Mingjie Xu[1†], Jiatong Zhou[1†], Jiancheng Lv[1*] and Yu Zhang[2*]

Abstract

Background Bladder cancer (BCa), a prevalent malignancy of the urinary tract, is associated with high recurrence and mortality rates. *SLC16A7*, a member of the solute carrier family 16 (SLC16), encodes monocarboxylate transporters that are involved in the proton-coupled transport of metabolites, including lactate, pyruvate, and ketone bodies, across cell membranes. Evidence suggests that *SLC16A7* exhibits variable expression in cancers and may influence tumor development, progression, and immune regulation. This study examined the role of *SLC16A7* in cancer prognosis, progression, and immune regulation, focusing on BCa.

Methods A comprehensive analysis was conducted to evaluate the clinical and immunological relevance of *SLC16A7* across multiple cancer types using data from 33 tumor datasets from 'The Cancer Genome Atlas (TCGA). ' Associations between *SLC16A7* expression and clinicopathological features, prognostic indicators, tumor mutation burden (TMB), microsatellite instability (MSI), immune cell infiltration, and immune-related gene expression were systematically analyzed. Experimental validation was performed to assess *SLC16A7* expression in the BCa tissues and cell lines. The prognostic value of *SLC16A7* was confirmed using clinical follow-up data from an independent patient cohort. Functional studies included proliferation assays to investigate the effect of *SLC16A7*. CD8 + T cells were obtained from the peripheral blood of healthy donors and stimulated using CD3 and CD28 antibodies in combination with recombinant IL-2. To investigate the immunological role of *SLC16A7*, co-culture experiments were performed between BCa cells and activated CD8 + T cells. Additionally, CD8 + T cell chemotaxis assays and ELISA analyses were conducted to evaluate the immune responses mediated by *SLC16A7*.

Results *SLC16A7* expression was downregulated in 16 cancer types, including BCa, and upregulated in three cancer types. Its expression was significantly associated with tumor stage in four cancers and showed both positive and negative correlations with prognosis, depending on the cancer type. Genomic analyses revealed significant associations between *SLC16A7* and TMB in 13 cancer types and MSI in 11 cancer types. Pathway enrichment analyses (Hallmark-GSEA and KEGG-GSEA) indicated strong associations between *SLC16A7*, immune responses, and tumor progression. Immune infiltration analysis showed a predominantly positive association between *SLC16A7* expression and immune cell infiltration, except in low-grade gliomas (LGG). CIBERSORT analysis demonstrated that

†Mingjie Xu and Jiatong Zhou contributed equally to this work.

*Correspondence:
Jiancheng Lv
1324089@zju.edu.cn
Yu Zhang
1028787131@qq.com

Full list of author information is available at the end of the article

SLC16A7 expression correlated positively with resting memory CD4 T cells, eosinophils, monocytes, resting mast cells, and memory B cells and negatively with activated memory CD4 T cells, M1 macrophages, follicular helper T cells, M0 macrophages, and CD8 T cells. *SLC16A7* expression was also significantly associated with the expression of immune-regulatory molecules. Experimental validation showed reduced *SLC16A7* expression in BCa tissues and cell lines compared to that in their normal counterparts. Kaplan-Meier survival analysis indicated that higher *SLC16A7* expression was correlated with better overall survival in patients with BCa. Functional assays revealed that *SLC16A7* inhibited BCa cell progression and promoted the chemotaxis and tumor-killing ability of CD8 + T cells in the BCa tumor microenvironment (TME).

Conclusions *SLC16A7* exhibits tumor-suppressive properties, with downregulation in most cancers, and is associated with favorable prognosis and enhanced immune responses. *SLC16A7* functions as a tumor suppressor in BCa and is associated with improved survival outcomes. These findings suggest that *SLC16A7* is a potential biomarker for cancer diagnosis and prognosis.

Keywords *SLC16A7*, Pan-cancer, Bladder cancer, Prognosis, Immune response

Introduction

Cancer remains one of the leading causes of mortality worldwide, and its heterogeneity necessitates ongoing exploration of novel biomarkers and therapeutic targets [1, 2]. Among these, metabolic reprogramming has emerged as a hallmark of cancer, with particular focus on metabolic enzymes and transporters that facilitate energy production and modulate the tumor microenvironment (TME) [3–5]. Bladder cancer (BCa) is among the most prevalent malignancies of the urinary tract and is characterized by high recurrence and notable mortality rates, particularly in advanced stages [6, 7]. As a highly heterogeneous disease with diverse molecular subtypes, BCa presents challenges for standardized treatment approaches [8, 9]. Traditional therapeutic options, including surgery, chemotherapy, and immunotherapy, have demonstrated limited long-term success, especially in patients with metastatic or recurrent forms of the disease [10, 11]. Consequently, there is a critical need to discover new molecular targets to facilitate the development of more effective therapeutic strategies.

The 'SLC16 gene family,' also known as 'monocarboxylate transporters (MCTs),' plays a crucial role in cellular metabolism and energy regulation [12]. Members of this family are responsible for the proton-coupled transport of key metabolic intermediates, such as lactate, pyruvate, and ketone bodies, across cell membranes [13]. These metabolites are essential for maintaining cellular homeostasis, particularly in tissues with high metabolic demands, such as tumors [14]. The SLC16 family consists of four isoforms, *SLC16A1*, *SLC16A3*, *SLC16A7*, and *SLC16A8*, each with distinct tissue expression patterns and functional roles [15]. These transporters are implicated in various physiological processes, including 'metabolic regulation,' 'pH homeostasis,' and cellular signaling' [13]. In the context of cancer, dysregulated expression of SLC16 family members has emerged as a significant factor in tumor progression and metabolism [14]. Tumors often exhibit 'altered metabolic pathways' to meet the high energy and biosynthetic demands required for rapid cell proliferation [16]. As part of this adaptive response, tumors frequently undergo aerobic glycolysis or the Warburg effect, where glucose is metabolized to lactate, even in the presence of oxygen [17, 18]. This shift in metabolism not only supports the anabolic needs of the tumor but also contributes to the acidic TME [19]. Interestingly, studies have also highlighted that the SLC16 gene family may alter immune cell metabolism and function by regulating metabolic fluxes, thereby influencing the tumor's ability to escape immune detection and destruction [20].

SLC16A7, also known as *MCT2*, is a prominent member of the SLC16 gene family and has been shown to display varying expression patterns and functions across different types of cancer [21, 22]. In prostate cancer, the localization of *SLC16A7* in peroxisomes has been linked to malignant transformation [23]. Conversely, in a murine model of lung cancer, *SLC16A7* was found to inhibit tumor growth [24]. Despite these findings, the role of *SLC16A7* in tumor immune evasion and local immune responses remains unclear. In this study, we examined the association between *SLC16A7* expression, clinical characteristics, and the prognosis in cancer patients. Additionally, we analyzed its effect on tumor immunity, including immune cell infiltration and the expression of immunomodulators and chemokines. Our findings revealed that *SLC16A7* was expressed at lower levels in most cancer types, and its expression influenced the prognosis of several cancers, generally enhancing the immune response. Further validation experiments demonstrated that *SLC16A7* expression was reduced in BCa and this downregulation was associated with better patient outcomes. The proliferation assay and immunological assays results revealed that *SLC16A7* inhibited the progression and promoted the immune response of BCa. This study identified *SLC16A7* as a potential novel biomarker for cancer diagnosis and prognosis.

Methods

Data collection and processing

RNA sequencing, clinical, and mutation data were retrieved from The Cancer Genome Atlas (TCGA) via UCSC Xena (https://xena.ucsc.edu/). *SLC16A7* expression data were extracted from these datasets using Strawberry Perl (version 5.32.0, available at http://strawberryperl.com/). Data preprocessing and further analyses were conducted using R software (version 4.0.2; https://www.Rproject.org).

Differential expression analysis

The expression of *SLC16A7* was evaluated in 24 normal and 33 cancerous tissue samples. The data were log2-transformed, and the expression levels of *SLC16A7* in the tumor samples were compared to those in the corresponding normal tissues. A T-test was used to assess significant differences in expression.

Clinical significance analysis

Correlations between *SLC16A7* expression and tumor stage were examined for each cancer type. The association between *SLC16A7* expression and various survival metrics, including overall survival (OS), disease-free survival (DFS), disease-specific survival (DSS), and progression-free survival (PFS) was explored. Kaplan-Meier curves were constructed for survival analysis for each cancer type.

Tumor mutation burden (TMB) and microsatellite instability (MSI) analysis

The association between *SLC16A7* expression and TMB and MSI across all tumor types was assessed using Spearman's rank correlation coefficient. TMB and MSI values were derived from mutation data.

Gene set enrichment analysis (GSEA)

GSEA was performed to assess the association between *SLC16A7* and all the genes using TCGA data. Both the KEGG-based and Hallmark-based GSEA analyses were conducted for various tumor types. The top five enriched pathways with the strongest correlations were identified and are presented.

Correlation between SLC16A7 and immune response

The ESTIMATE algorithm was used to calculate the immune and stromal scores of tumors, providing insights into their immune landscape. The association between *SLC16A7* expression and immune scores across different tumor types was analyzed using the R software. CIBERSORT, a metagene analysis tool, was used to determine the infiltration scores of 26 distinct immune cell types within each tumor sample. The association between *SLC16A7* expression and immune cell infiltration scores was calculated using R. Additionally, correlations between *SLC16A7* and various immune-related features, such as lymphocyte infiltration, immunoinhibitors, immunostimulators, MHC molecules, chemokines, and chemokine receptors, were explored using the TISIDB website (http://cis.hku.hk/TISIDB/).

Patient tissues and cell lines

Twenty pairs of BCa tissues and adjacent normal tissues were collected from patients undergoing radical cystectomy at the First Affiliated Hospital of Zhejiang University School of Medicine (Hangzhou, China) between 2018 and 2023. Informed consent was obtained from all patients. The use of these tissue samples was approved by the Ethics Committee of the First Affiliated Hospital of the Zhejiang University School of Medicine. BCa tissues were pathologically confirmed and adjacent normal tissues were diagnosed as non-tumorous. Several BCa cell lines (T24, UMUC3, 253 J, 5637, J82, BIU87, and RT4) and a normal urothelial cell line (SV-HUC) were obtained from the Type Culture Collection of the Chinese Academy of Sciences (Shanghai, China).

Human protein atlas (HPA)

The protein expression of *SLC16A7* in BCa and normal urothelial tissues was investigated using the Human Protein Atlas database (https://www.proteinatlas.org/).

RNA isolation and quantitative Real-Time PCR (qRT-PCR)

RNA was extracted from BCa tissues or cells using TRIzol reagent (Invitrogen, USA). RNA concentration was measured using a microplate reader (Tecan, Switzerland), and cDNA synthesis was carried out using the HiScript II reagent (Vazyme, China). For qRT-PCR, the reaction mixture was prepared using a SYBR premix kit (Vazyme, Nanjing, China). Amplification was performed using a StepOne Plus real-time PCR system (Applied Biosystems, USA). The relative expression of the target gene was normalized to that of β-actin by subtracting its CT value from the CT value of the target gene. The primers used in this study were designed and sourced from TsingKe (Table S1).

Cell culture and transfection

T24 and UMUC3 cells were cultured in DMEM (Gibco, USA) supplemented with 10% fetal bovine serum (BI, Israel) and incubated at 37 °C with 5% CO_2. To silence *SLC16A7* expression, small interfering RNA (siRNA) specific to *SLC16A7* and a control vector were purchased from GenePharma (Shanghai, China). To overexpress *SLC16A7* expression, overexpression plasmid and relative control vector were also purchased from GenePharma (Shanghai, China). When cells reached 50% confluence in six-well plates, they were transfected with siRNAs or

overexpression plasmid using the Lipofectamine 3000 kit (Invitrogen, USA).

Cell proliferation assay

To assess the effect of *SLC16A7* on cell proliferation, 3,000 UMUC3 cells or 2,000 T24 cells were seeded in 96-well plates. Cell viability was evaluated every 24 h (at 24, 48, 72, and 96 h) using a Cell Counting Kit-8 (CCK-8, Dojindo, Japan). After replacing the medium in each well with fresh medium containing 10 µL of the CCK-8 reagent, the cells were incubated for one hour. The absorbance was measured at 450 nm using a microplate reader (Tecan, Switzerland).

Colony formation assay

T24 or UMUC3 cells (1,000 and 1,500, respectively) were seeded in 12-well plates. After culturing for two weeks, cell colonies were fixed using 4% paraformaldehyde for 20 min and then stained with 0.1% crystal violet for 20 min. After washing with PBS for several times, colony counts were obtained using ImageJ software.

Isolation, activation, and culture of CD8 + T cells

Peripheral blood mononuclear cells (PBMCs) were extracted from the blood of healthy donors using a PBMC isolation reagent (FACs; Nanjing, China). CD8 + T cells were subsequently purified from the PBMCs via CD8 microbeads (Miltenyi, Germany). The isolated CD8 + T cells were then cultured in RPMI-1640 medium (Gibco, USA) and stimulated for 72 h with CD3 antibodies (2 µg/mL; Invitrogen, USA), CD28 antibodies (1 µg/mL; Invitrogen, USA), and recombinant interleukin-2 (IL-2; 5 ng/mL; R&D Systems, USA).

Chemotaxis and CD8 + T-Cell antitumor activity assay

A chemotaxis assay was performed using a Transwell insert with 3 µm pores (Corning, USA) in a 24-well plate. Approximately 4×10^5 activated CD8 + T cells were loaded into the upper chamber, while 1×10^5 bladder cancer (BCa) cells were placed in the lower chamber. After 24 h, the number of CD8 + T cells that migrated to the lower chamber was quantified using the CCK-8 assay. Following 72 h of co-culture, the supernatant was collected, IFN-γ and granzyme B levels were measured using ELISA kits (FACs, Nanjing, China).

Statistical analysis

Data were analyzed using SPSS (version 22.0; IBM Corp., Armonk, NY, USA) and expressed as mean ± standard deviation (mean ± SD). Differences between groups were determined using Student's t-test or one-way analysis of variance (ANOVA). Statistical significance was defined as a *P*-value of less than 0.05.

Results

Pan-Cancer expression analysis of SLC16A7

The expression levels of *SLC16A7* in various cancer types were analyzed using data from TCGA. *SLC16A7* expression was significantly lower in 16 tumor types, including bladder cancer (BLCA), breast cancer (BRCA), colon cancer (COAD), esophageal carcinoma (ESCA), glioblastoma (GBM), head and neck squamous carcinoma (HNSC), kidney renal clear cell carcinoma (KIRC), kidney renal papillary cell carcinoma (KIRP), lung squamous cell carcinoma (LUSC), pheochromocytoma (PCPG), prostate cancer (PRAD), rectal adenocarcinoma (READ), stomach cancer (STAD), thyroid cancer (THCA), thymoma (THYM), and uterine corpus endometrial carcinoma (UCEC), than in the corresponding normal tissues. In contrast, *SLC16A7* was upregulated in cholangiocarcinoma (CHOL), kidney chromophobe (KICH), and lung adenocarcinoma (LUAD) compared to normal tissues (Fig. 1A). Overall, *SLC16A7* expression was significantly lower in the tumor tissues than in the adjacent normal tissues (Fig. 1B). Analysis of *SLC16A7* expression across various stages of tumor progression revealed higher expression in stage I for adrenal carcinoma (ACC), BRCA, and HNSC, whereas it was lower in stage I for liver hepatocellular carcinoma (LIHC) (Fig. 1C). Additionally, the expression of *SLC16A7* was highest in KICH, acute myeloid leukemia (LAML), and ACC, whereas it was lower in UCEC, READ, and ovarian cancer (OV) (Fig. 1D).

Prognostic implications of SLC16A7 in Pan-Cancer

To explore the potential role of *SLC16A7* in cancer prognosis, we performed survival analyses including OS, DFS, DSS, and PFS across various cancer types. Cox proportional hazards model analysis revealed that *SLC16A7* expression was significantly associated with OS in ACC, LGG, STAD, and THYM, acting as a high-risk factor in STAD and a low-risk factor in ACC, LGG, and THYM (Fig. 2A). Kaplan-Meier survival curves showed that high *SLC16A7* expression correlated with better OS in ACC and THYM, whereas it was associated with poorer OS in cervical squamous cell carcinoma (CESC) and STAD (Fig. 2B-E). Further Cox analysis indicated that *SLC16A7* was also significantly associated with DFS in ESCA and STAD, where it served as a high-risk gene for both (Figure S1A), with Kaplan-Meier survival curves confirming that high *SLC16A7* expression in STAD was correlated with worse DFS (Figure S2B). In terms of DSS, *SLC16A7* was associated with outcomes in ACC, LGG, STAD, THYM, and UCEC, acting as a high-risk gene in STAD and UCEC but a low-risk gene in ACC, LGG, and THYM (Figure S2A). Kaplan-Meier analyses further showed that high *SLC16A7* expression improved DSS in THYM, but worsened DSS in CESC and STAD (Figure S2B-D).

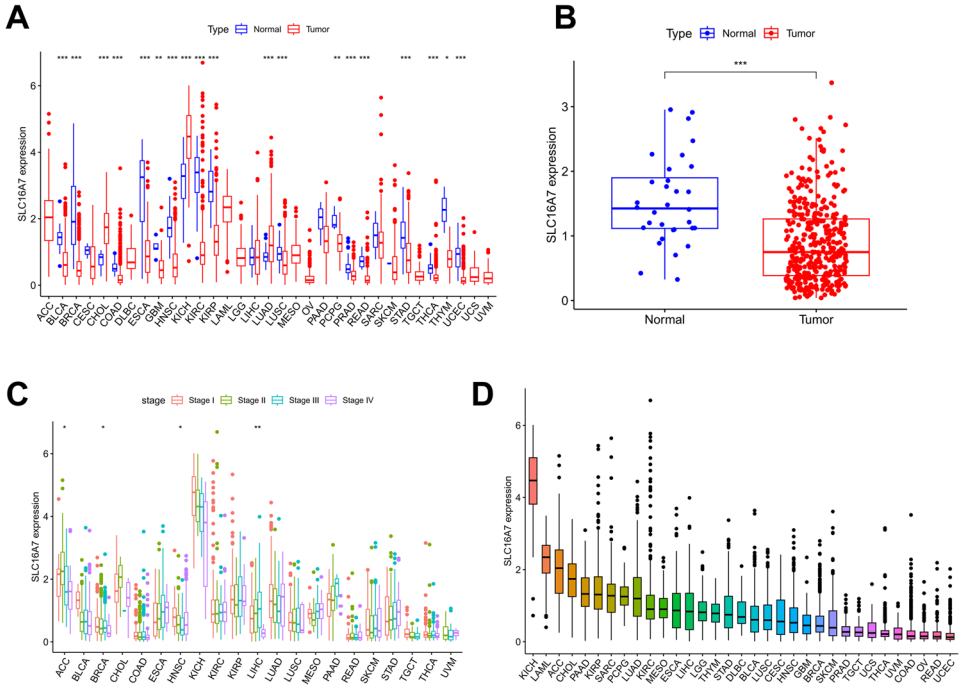

Fig. 1 Expression of *SLC16A7* Across TCGA Pan-Cancer Types. **A**. Expression levels of *SLC16A7* in various TCGA pan-cancer types compared to normal tissues (*$P < 0.05$, **$P < 0.01$, ***$P < 0.001$, Student's t-test). **B**. Overall expression of *SLC16A7* in tumor vs. normal tissues across all cancers (***$P < 0.001$, Student's t-test). **C**. Expression variation of *SLC16A7* in different stages of various cancers (*$P < 0.05$, **$P < 0.01$, Student's t-test). **D**. Expression of *SLC16A7* in 31 different tumor types

PFS analysis revealed a significant association between *SLC16A7* and PFS in ACC, LGG, STAD, and UCEC, where it acted as a high-risk gene in STAD and UCEC, but as a low-risk factor in ACC and LGG (Figure S3A). Kaplan-Meier curves confirmed that high *SLC16A7* expression correlated with better PFS in LGG but worse PFS in CESC and STAD (Figure S3B-D).

Correlation of SLC16A7 with TMB and MSI

The association between *SLC16A7* expression and TMB or MSI across various cancers was analyzed. *SLC16A7* was significantly correlated with TMB in 13 tumor types, including ACC, BCa, BRCA, COAD, ESCA, KIRP, LAML, LUAD, LUSC, PAAD, PRAD, STAD, and THYM (Fig. 3A). *SLC16A7* was significantly associated with MSI in 11 cancer types, including BCa, COAD, diffuse large B-cell lymphoma (DLBC), GBM, HNSC, LUSC, PAAD, PRAD, READ, skin cutaneous melanoma (SKCM), and STAD (Fig. 3B).

GSEA of SLC16A7

To examine the biological roles of *SLC16A7* in different cancers, we performed KEGG-GSEA and Hallmarks-GSEA analyses. The KEGG pathway gene sets and Hallmark pathway gene sets were downloaded from [GSEA-MSIGDB](https://www.gsea-msigdb.org/gsea/index.jsp). The KEGG-GSEA results revealed that *SLC16A7* was positively correlated with cancer and immune-related pathways, including antigen processing and presentation, chemokine signaling, cytokine-cytokine receptor interactions, NK cell-mediated cytotoxicity, cancer pathways, and JAK-STAT signaling, across 14 tumor types. It was negatively correlated with immune-regulatory pathways in both cancer types (Fig. 4). Similarly, Hallmarks-GSEA indicated that *SLC16A7* was positively associated with immune-related pathways, including the IL6-JAK-STAT3 signaling pathway, inflammatory response, interferon gamma response, TNFA signaling via NFkB, IL2-STAT5 signaling, and complement pathways in 11 tumors, with a negative correlation in only one cancer type (Fig. 5).

Immune response correlation with SLC16A7 expression in Pan-Cancer

SLC16A7 expression and its association with immune cell infiltration were assessed using the ESTIMATE algorithm to calculate the immune scores. *SLC16A7* was positively correlated with immune scores in 14 cancer types, including BRCA, COAD, HNSC, LUAD, LUSC, OV, PAAD, PRAD, READ, SKCM, STAD, THCA, UCEC, and UCS, but negatively associated with LGG (Fig. 6). CIBERSORT analysis further revealed a positive correlation between *SLC16A7* expression and resting memory CD4 + T cells, eosinophils, monocytes, resting mast cells, and memory B cells, whereas it was inversely correlated with activated memory CD4 + T cells, M1 macrophages, follicular helper T cells, M0 macrophages, and

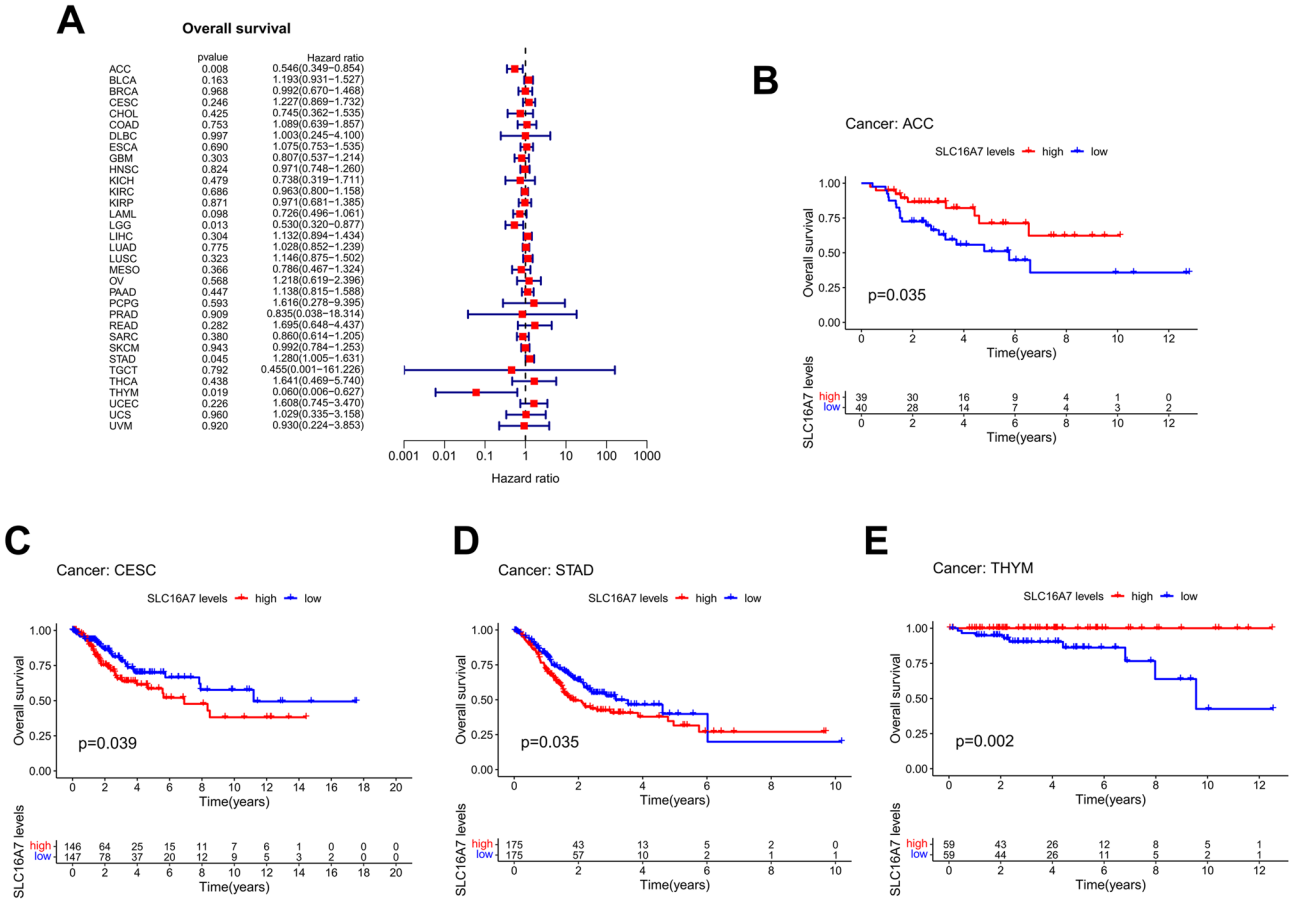

Fig. 2 *SLC16A7*'s Impact on Overall Survival Across TCGA Pan-Cancer. **A**. Cox proportional hazards model showing the association between *SLC16A7* and overall survival (OS) in pan-cancer. **B**-**E**. Kaplan-Meier survival analysis depicting the correlation between *SLC16A7* expression and OS in various tumor types

CD8 + T cells (Fig. 7). Co-expression analysis indicated that *SLC16A7* was generally positively correlated with immune response genes, including those related to lymphocyte infiltration, immunoinhibitors, immunostimulators, MHC molecules, chemokines, and chemokine receptors in most cancers, except for LGG, SARC, and UVM (Fig. 8).

SLC16A7 expression in BCa tissues and cell lines

In bladder cancer, the expression of *SLC16A7* was significantly lower in tumor tissues than in adjacent normal tissues, as confirmed by qRT-PCR in 20 pairs of BCa samples (Fig. 9A). Additionally, six BCa cell lines (BIU87, T24, J82, 5637, UMUC3, and RT4) exhibited reduced *SLC16A7* expression compared with the normal urothelial cell line SV-HUC (Fig. 9B). HPA further confirmed the low expression of *SLC16A7* in BCa tissues (Fig. 9C). Kaplan-Meier survival analysis indicated that higher *SLC16A7* expression was associated with improved OS in patients with BCa (Fig. 9D).

Impact of SLC16A7 on BCa cell proliferation

To assess the functional role of *SLC16A7*, siRNAs targeting *SLC16A7* were transfected into the T24 and UMUC3 BCa cell lines. Successful knockdown of *SLC16A7* was confirmed by qRT-PCR (Fig. 10A-B). The results of CCK-8 assays demonstrated that silencing *SLC16A7* significantly promoted cell proliferation in both T24 and UMUC3 cell lines (Fig. 10C-D). The results of Colony formation assays confirmed that silencing *SLC16A7* significantly promoted cell proliferation in both T24 and UMUC3 cell lines (Fig. 10E-F). To further assess the functional role of *SLC16A7*, *SLC16A7* overexpression plasmid was transfected into the T24 and UMUC3 BCa cell lines. Successful overexpression of *SLC16A7* was confirmed by qRT-PCR (Fig. 11A). The results of CCK-8 assays demonstrated that *SLC16A7* overexpression significantly inhibited cell proliferation in both T24 and UMUC3 cell lines (Fig. 11B). The results of Colony formation assays confirmed that *SLC16A7* overexpression significantly inhibited cell proliferation in both T24 and UMUC3 cell lines (Fig. 11C).

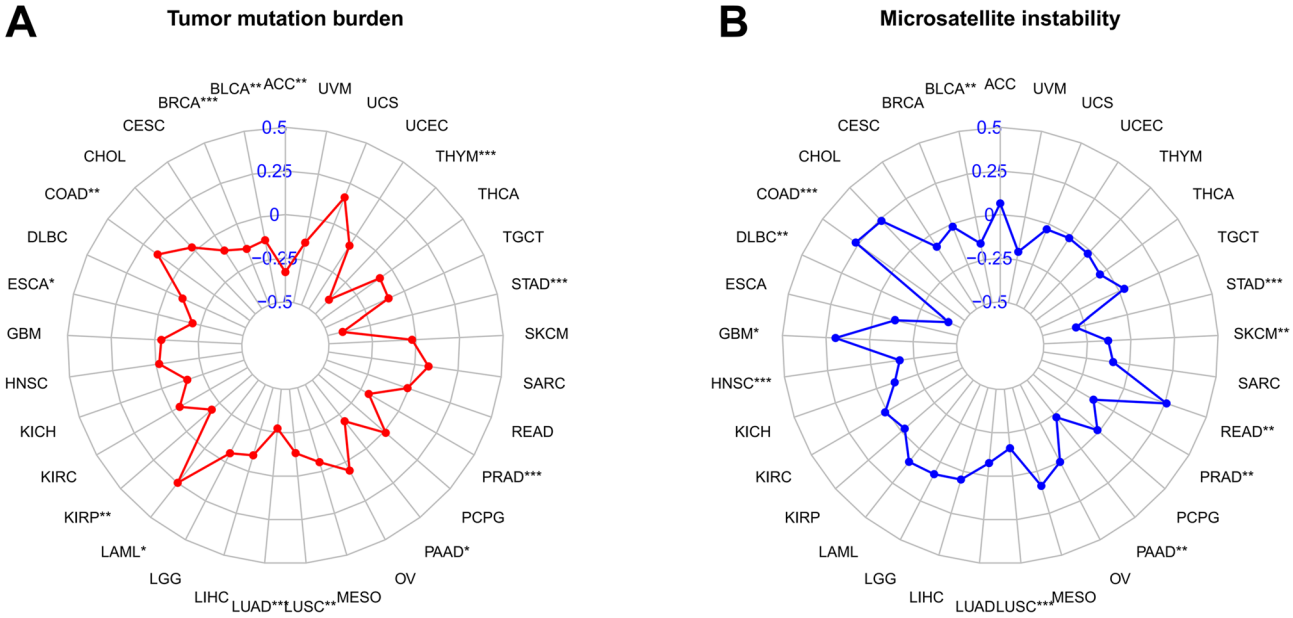

Fig. 3 *SLC16A7* and Its Associations with TMB and MSI in TCGA Pan-Cancer. **A**. Correlation between *SLC16A7* expression and tumor mutation burden (TMB) across different cancers (**P* < 0.05, ***P* < 0.01, ****P* < 0.001, Student's t-test). **B**. Correlation between *SLC16A7* and microsatellite instability (MSI) in various cancers (**P* < 0.05, ***P* < 0.01, ****P* < 0.001, Student's t-test)

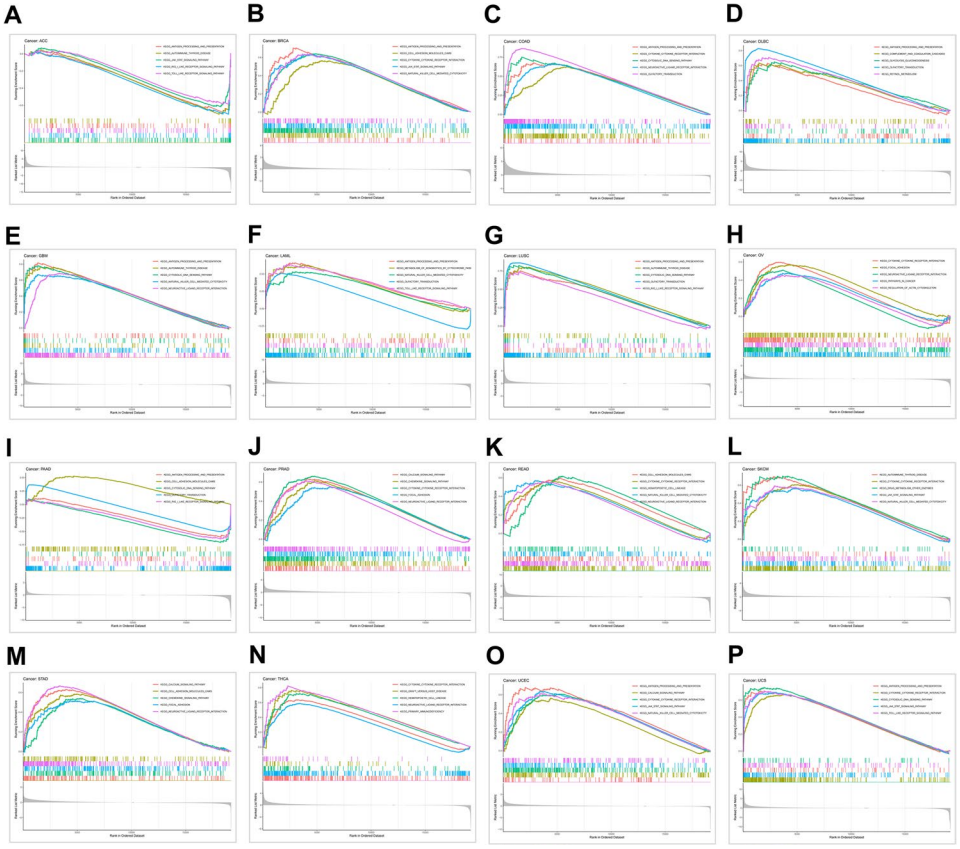

Fig. 4 KEGG-GSEA Analysis of *SLC16A7* in TCGA Pan-Cancer. **A**-***P***. KEGG pathway analysis of *SLC16A7* in various tumor types, highlighting its enrichment in pathways related to tumor progression and immune response

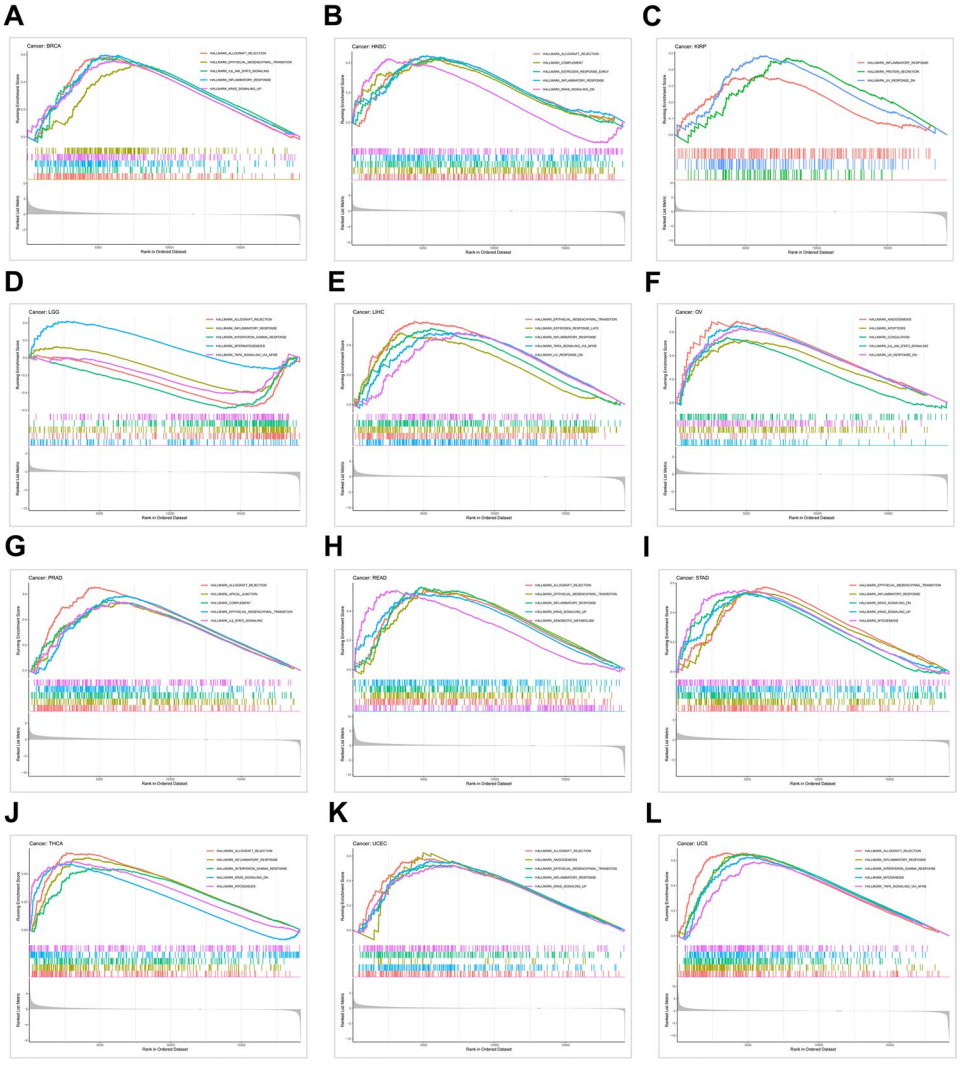

Fig. 5 Hallmarks-GSEA Analysis of *SLC16A7* in TCGA Pan-Cancer. **A**-**L**. Hallmark pathway analysis showing *SLC16A7*'s association with immune response pathways across different cancer types

SLC16A7 overexpression promoted the chemotaxis and antitumor function of CD8$^+$ T cells in BCa TME

CD8 + T cells were isolated from the peripheral blood of healthy individuals and activated by culture in RPMI-1640 medium supplemented with CD3, CD28, and IL-2 antibodies. To assess the function of *SLC16A7* on CD8 + T-cell chemotaxis, a two-chamber co-culture model was established (Fig. 11D). Co-culturing *SLC16A7* overexpression T24 or UMUC3 cells with activated CD8 + T cells led to enhanced movement of CD8 + T cells to the lower chamber (Fig. 11E). After 72 h, the medium from the co-culture system was obtained for ELISA assays to measure IFN-γ and granzyme B production by activated CD8 + T cells. The results revealed that co-culture with *SLC16A7* overexpression T24 or UMUC3 cells enhanced IFN-γ and granzyme B production of CD8 + T cells (Fig. 11F). Thus, *SLC16A7* promotes the chemotaxis and antitumor function of CD8 + T cells in the BCa TME.

Discussion

This study investigated the expression and functional significance of *SLC16A7*, a gene encoding a monocarboxylate transporter, in BCa and across various cancers. *SLC16A7* is involved in the proton-coupled transport of critical metabolites, such as lactate, pyruvate, and ketone bodies, which are integral to cellular metabolism and TME dynamics [12]. Although its role in metabolic regulation is well established, its involvement in tumor progression, prognosis, and immune evasion remains unclear. Our study aimed to address this gap by analyzing *SLC16A7* expression, its association with clinical tumor significance and immune response, and its potential as a biomarker and therapeutic target, particularly for BCa. Our results demonstrate that *SLC16A7* is broadly downregulated in 16 cancer types, including BCa, but upregulated in 3 tumor types. Database analysis revealed that *SLC16A7* is closely associated with clinical significance,

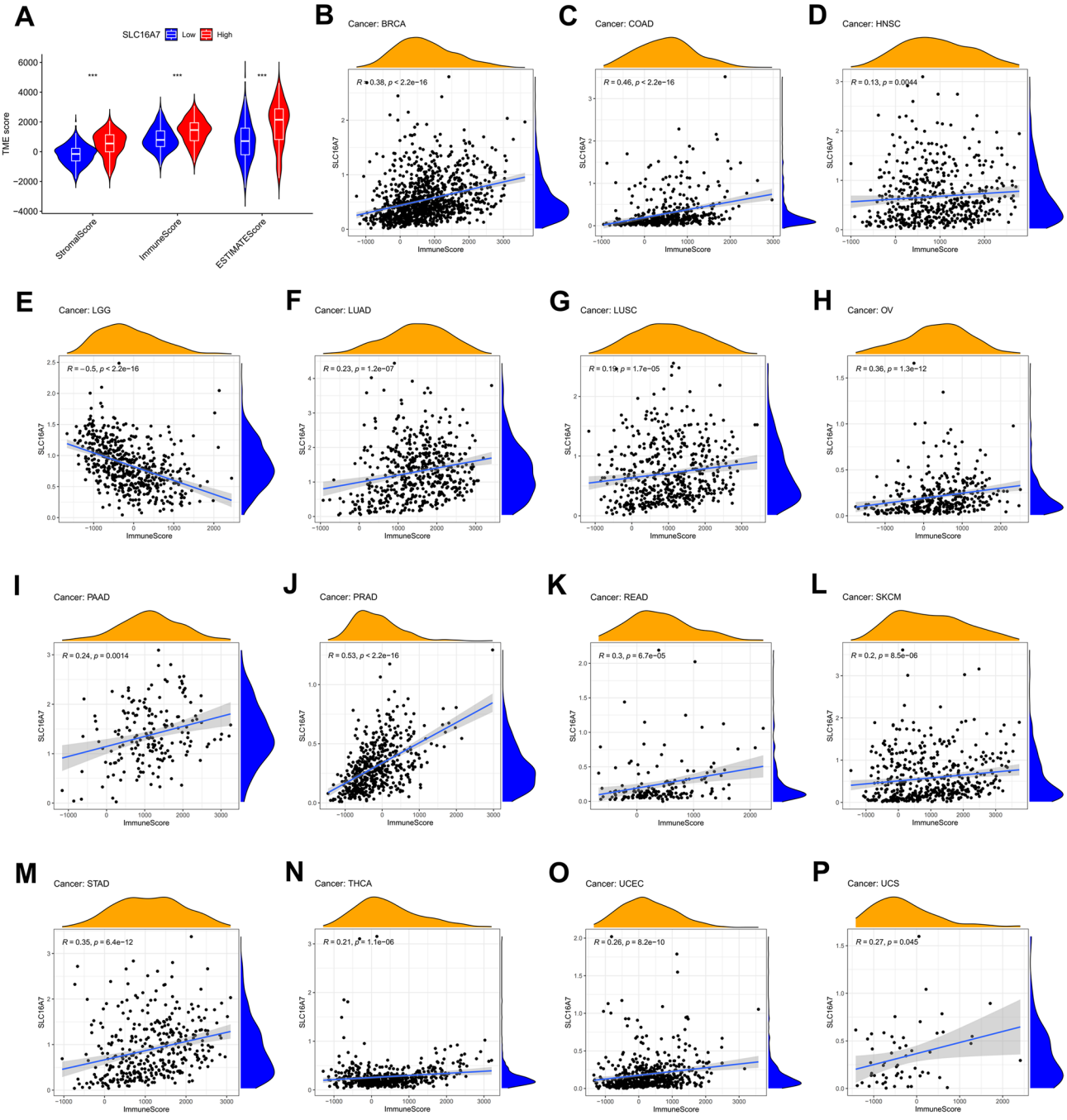

Fig. 6 Immune Scores and *SLC16A7* Expression Across TCGA Pan-Cancer. **A**. Correlation between *SLC16A7* expression and immune scores in TCGA pan-cancer. **B**-***P***. Correlations between *SLC16A7* and immune scores in individual cancer types

TMB, MSI, immune cell infiltration, and immune response genes in a variety of cancers, including BCa. Furthermore, Hallmark and KEGG enrichment analyses demonstrated that *SLC16A7* was positively correlated with immune response-related signaling pathways, such as the inflammatory response pathway, in most cancer types. Specifically, experimental validation confirmed that *SLC16A7* expression was markedly lower in BCa tissues and cell lines than that in adjacent normal tissues and urothelial cell lines. Kaplan-Meier analysis revealed that BCa patients with elevated *SLC16A7* expression exhibited improved OS. Proliferation assays and immunological assays indicated that *SLC16A7* acts as a tumor suppressor in BCa. Our findings highlight the potential value of *SLC16A7* as a novel biomarker and therapeutic target for cancer. These results also suggest that *SLC16A7* may modulate tumor immunity, potentially influencing the TME to suppress immune evasion.

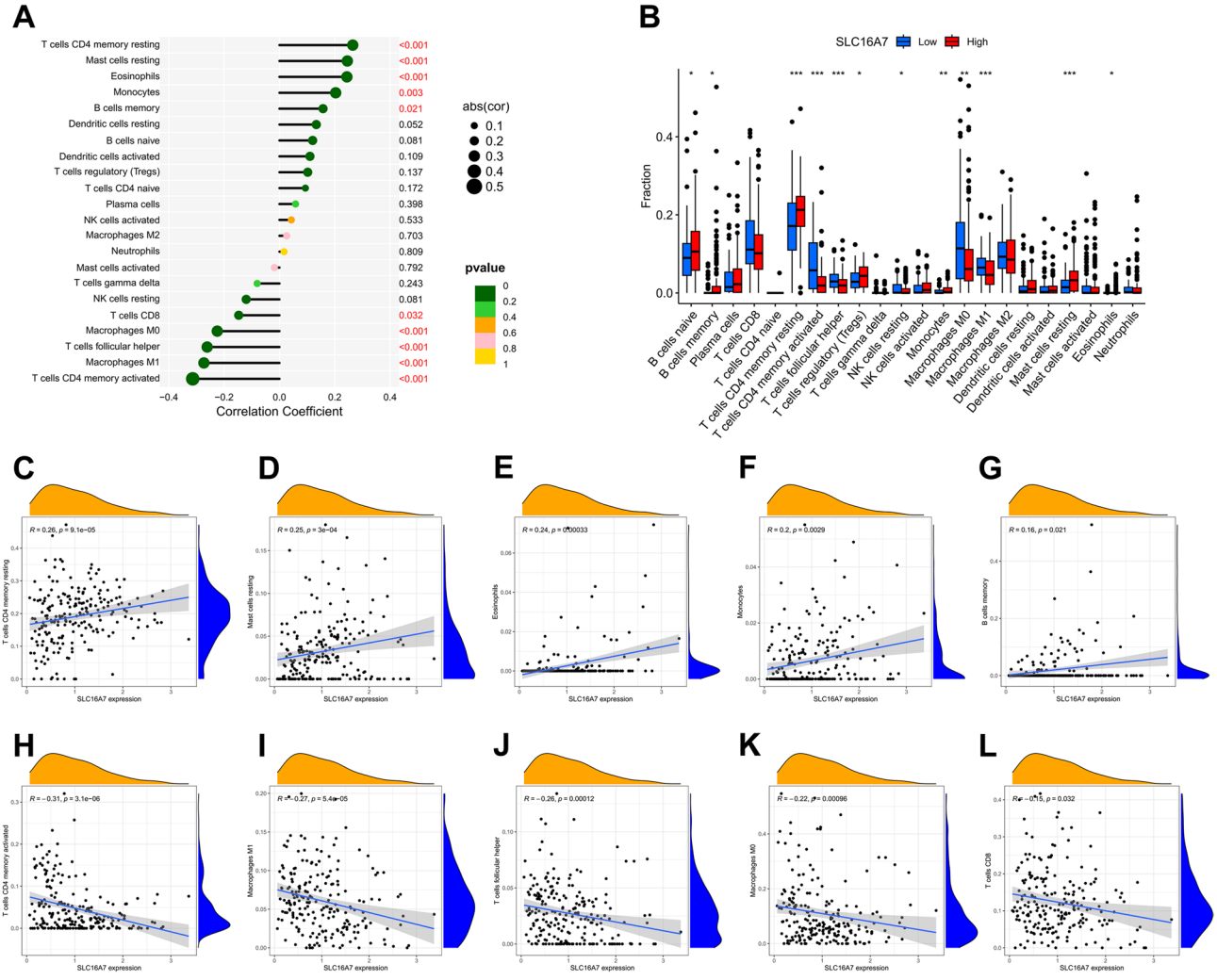

Fig. 7 *SLC16A7* and Immune Cell Infiltration in Various Cancers. **A**. Analysis of the correlation between *SLC16A7* expression and immune cell infiltration across TCGA pan-cancer. **B**. Immune cell infiltration in high and low *SLC16A7* expression groups across cancers. **C**-**G**. Correlation between *SLC16A7* and specific immune cells such as resting memory CD4 T cells, eosinophils, monocytes, resting mast cells, and memory B cells. **H**-**L**. Correlation between *SLC16A7* and immune cells like activated memory CD4 T cells, M1 macrophages, follicular helper T cells, M0 macrophages, and CD8 T cells

Recent studies have highlighted the dysregulated expression of members of the SLC16 gene family, including *SLC16A1*, *SLC16A7*, and *SLC16A3*, in various cancers, suggesting their roles in tumor progression and metastasis [14, 25]. *SLC16A1* is upregulated in several cancers, including glioma, breast cancer, cholangiocarcinoma, gastric cancer, oral cancer, lymphoma, skin squamous cell carcinoma, soft tissue sarcoma, and non-small cell lung cancer [26–34], whereas it is downregulated in prostate cancer [35]. *SLC16A3* is elevated in cancers such as breast, esophageal, oral, non-small cell lung, osteosarcoma, and liver cancer [28, 31, 33, 36–39], whereas it is downregulated in diffuse large B-cell lymphoma and Burkitt lymphoma [29]. *SLC16A7* is upregulated in breast, lung, and prostate cancers [28, 35], whereas its expression is low in hepatocellular carcinoma [40]. SLC16 transporters mediate lactate transport, which plays a crucial role in the metabolic symbiosis between glycolytic and oxidative cancer cells, facilitating tumor growth [41]. Lactate exported by glycolytic cancer cells is utilized by oxidative cancer cells, which supports their oxidative metabolism [41]. Additionally, lactate transport by SLC16 transporters promotes angiogenesis by activating the *HIF-1α* and *NF-κB* pathways, which enhance the expression of pro-angiogenic factors such as *VEGF-A* and *IL-8* [42–48]. Given their pivotal roles in cancer progression, SLC16 transporters represent promising therapeutic targets, and inhibitors such as CHC and AZD3965 are being explored in clinical trials as potential cancer treatments [14, 15, 49, 50]. Our findings demonstrate that *SLC16A7* is predominantly downregulated in tumors and is positively correlated with favorable prognosis. This disparity highlights the distinct functional roles of the individual SLC16 family members in cancer biology.

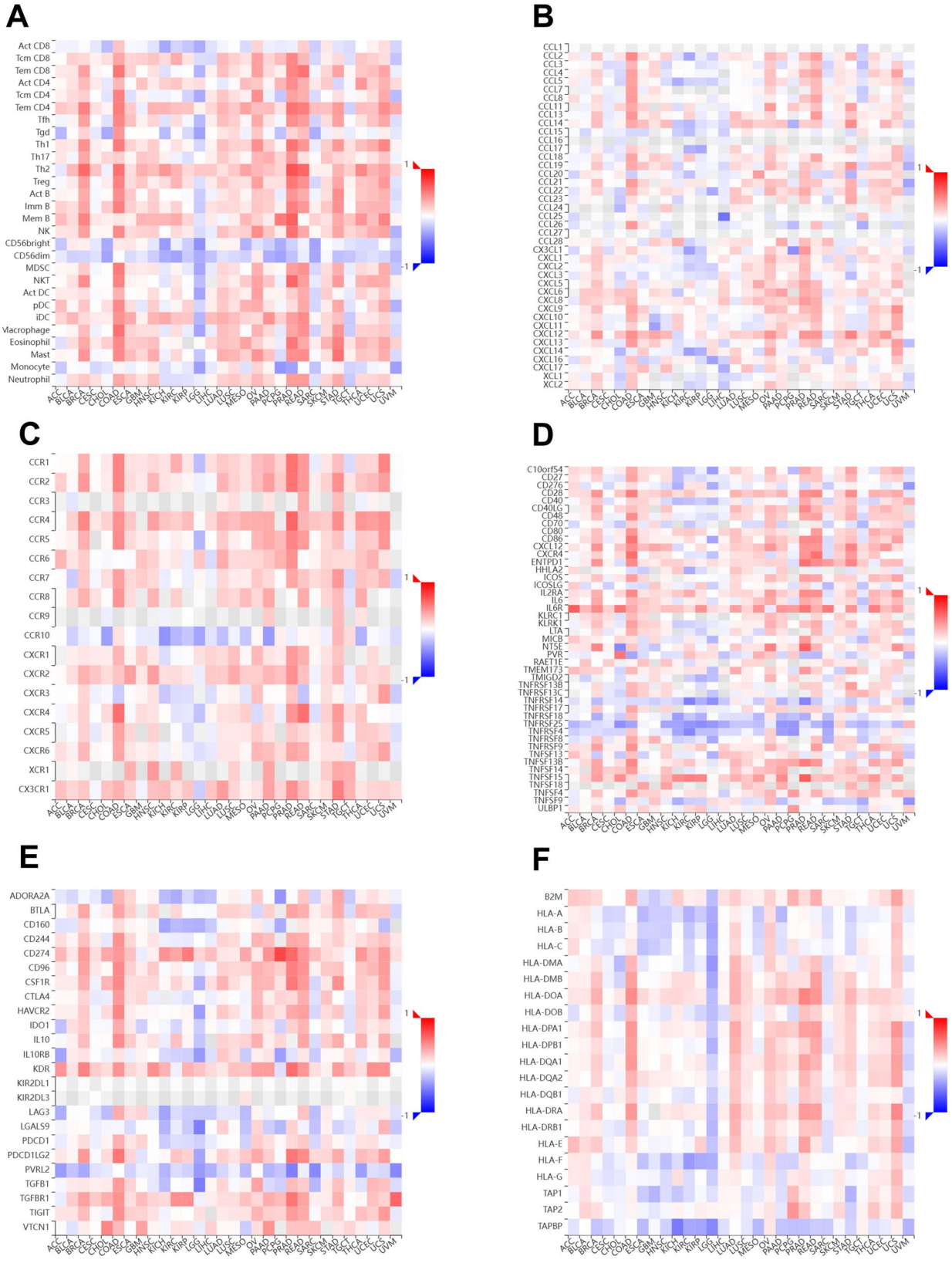

Fig. 8 *SLC16A7* and Immune Response-Related Genes in Pan-Cancer. **A**. Associations between *SLC16A7* and infiltrated immune cells across various cancers in TCGA. **B**. Relationship between *SLC16A7* expression and chemokine genes in TCGA pan-cancers. **C**. Correlation between *SLC16A7* and chemokine receptors across TCGA pan-cancers. **D**. Associations between *SLC16A7* and immunostimulatory genes in TCGA pan-cancers. **E**. *SLC16A7*'s association with immune inhibitors in TCGA pan-cancers. **F**. Correlation between *SLC16A7* and MHC molecules across various cancer types in TCGA

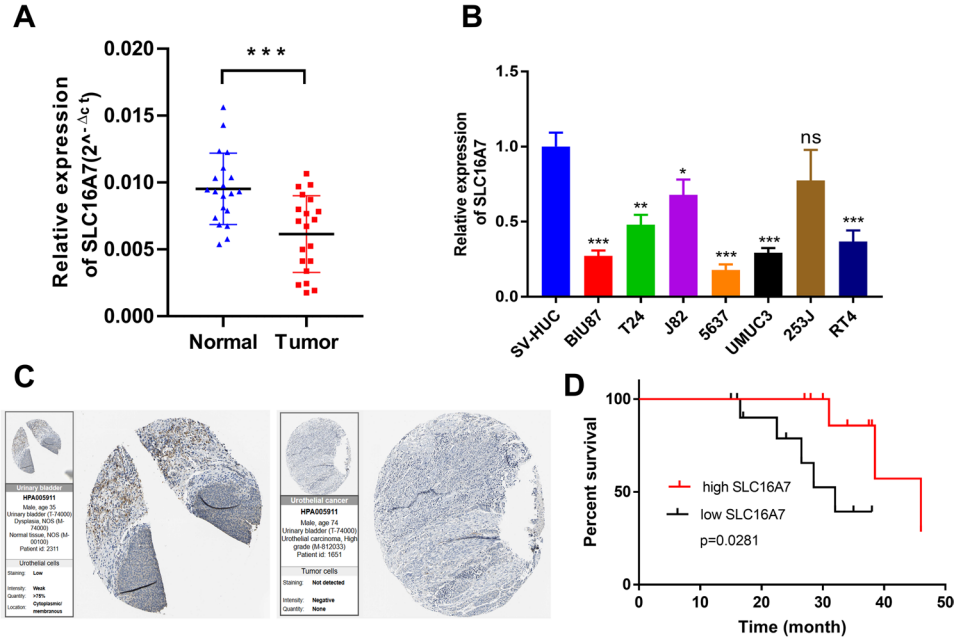

Fig. 9 Low Expression of *SLC16A7* in Bladder Cancer (BCa). **A**. *SLC16A7* expression in 20 pairs of BCa tissues, confirmed by qRT-PCR (***$P < 0.001$, Student's t-test). **B**. *SLC16A7* expression in BCa cell lines compared to SV-HUC, validated by qRT-PCR (*$P < 0.05$, **$P < 0.01$, ***$P < 0.001$, Student's t-test). **C**. HPA database validation of *SLC16A7* expression in BCa vs. normal tissues. **D**. Kaplan-Meier survival analysis correlating *SLC16A7* expression with overall survival in 20 BCa patients. Data presented as mean ± SD, $n = 3$

In terms of immune regulation, there is limited evidence linking *SLC16A7* to immune response. However, recent advances in cancer research have highlighted the essential role of SLC16 transporters in tumor immune responses. For example, SLC16 transporters could contribute to immune evasion by suppressing T and NK cell functions in the TME [51]. Another study emphasized the critical role of *SLC16A3* (*MCT4*)-mediated lactate efflux in shaping the immunosuppressive TME, and demonstrated that targeting *SLC16A3* can enhance the effectiveness of immunotherapy by reversing glycolysis-driven resistance mechanisms [52]. Understanding the function of specific metabolic transporters within the TME could offer valuable insights into cancer immunology and open new avenues for therapeutic interventions. Our study provides critical insights into the contribution of *SLC16A7* to immune cell infiltration and immune response regulation, particularly its positive association with key immune cell populations and immunomodulators. These findings expand the current understanding of *SLC16A7*'s functional relevance beyond metabolic transport, and position it as a key player in immune oncology.

Despite these promising findings, this study had some limitations. First, reliance on publicly available datasets, such as TCGA, introduces potential biases related to sample heterogeneity and data quality. The experimental validation of the observed correlations was limited to BCa, and further studies are needed to confirm these findings in other cancers.

Conclusions

In conclusion, *SLC16A7* is differentially expressed in many tumors and significantly correlated with tumor prognosis and immune response. *SLC16A7* is down-regulated and positively associated with prognosis in BCa. *SLC16A7* could inhibit the progression and enhance the immune response of BCa. *SLC16A7* shows great potential as a diagnostic, prognostic, and immunotherapeutic biomarker.

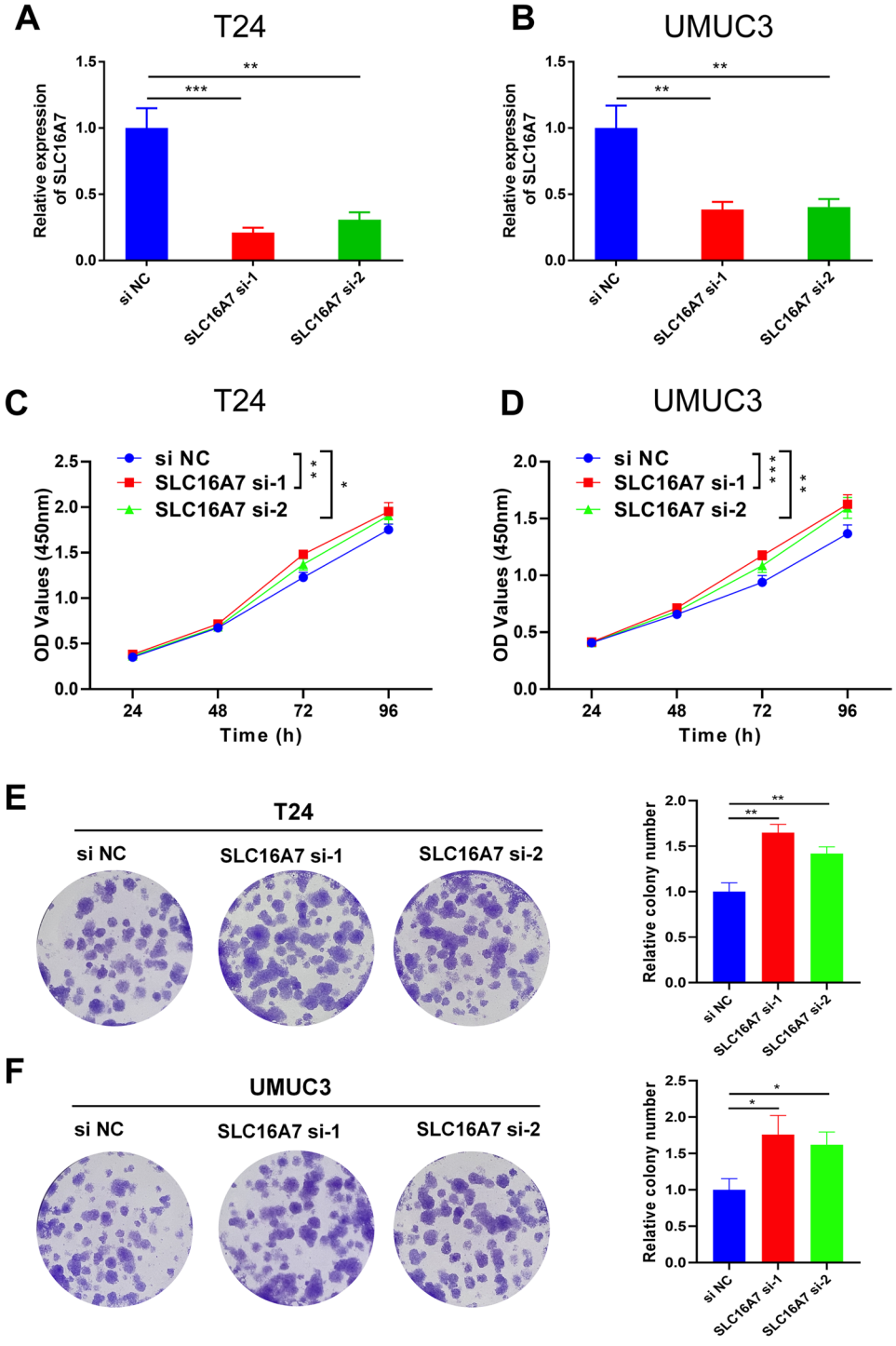

Fig. 10 Effect of *SLC16A7* Knockdown on BCa Cell Proliferation. **A**-**B**. Validation of *SLC16A7* knockdown efficiency in T24 and UMUC3 cells by qRT-PCR (***P* < 0.01, ****P* < 0.001, Student's t-test). **C**-**D**. CCK-8 assay confirming that *SLC16A7* inhibition enhances proliferation of T24 and UMUC3 cells (**P* < 0.05, ***P* < 0.01, *****P* < 0.0001, Student's t-test). **E**-**F**. Colony formation assay confirming *SLC16A7* inhibition enhances proliferation of T24 and UMUC3 cells (**P* < 0.05, ***P* < 0.01, Student's t-test). Data presented as mean ± SD, *n* = 3

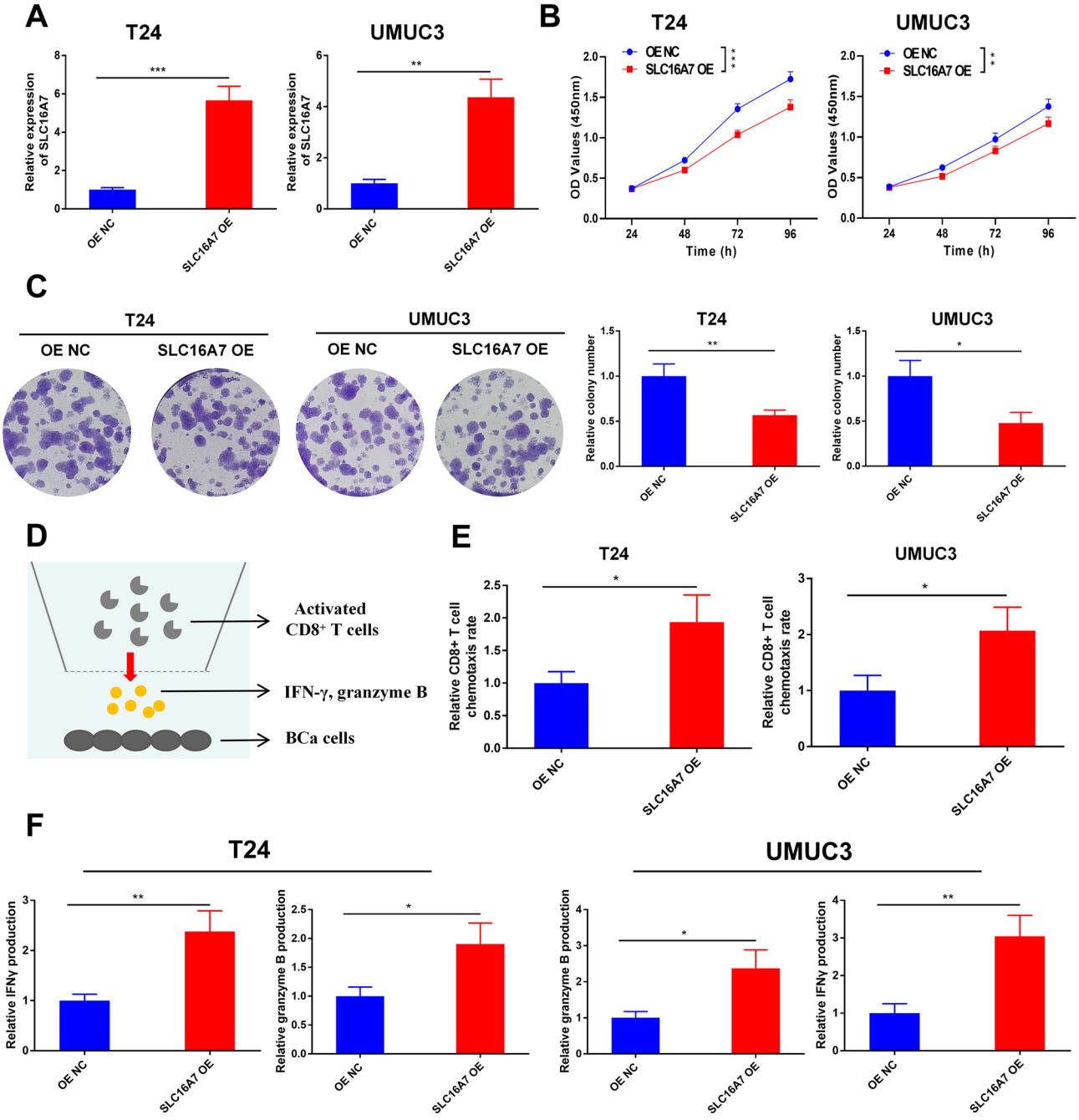

Fig. 11 Effect of *SLC16A7* overexpression on BCa Cell Proliferation and immune response. **A**. Validation of *SLC16A7* overexpression efficiency in T24 and UMUC3 cells by qRT-PCR (***P* < 0.01, ****P* < 0.001, Student's t-test). **B**. CCK-8 assay confirming that *SLC16A7* overexpression inhibits proliferation of T24 and UMUC3 cells (***P* < 0.01, *****P* < 0.0001, Student's t-test). **C**. Colony formation assay confirming *SLC16A7* overexpression inhibits proliferation of T24 and UMUC3 cells (**P* < 0.05, ***P* < 0.01, Student's t-test). **D**. Schematic diagram of the CD8 + T cell-BCa cell co-culturing assay. **E**. Chemotaxis assays revealed that CD8 + T cell chemotaxis was enhanced when were co-culturing with *SLC16A7* overexpression cells (**P* < 0.05, Student's t test). **F**. ELISA results revealed that CD8 + T cells produced more IFN-γ and granzyme B when co-culturing with *SLC16A7* overexpression BCa cells (**P* < 0.05, ***P* < 0.01, Student's t test). Data presented as mean ± SD, *n* = 3

Abbreviations

SLC16A7	Solute Carrier Family 16 Member 7
TCGA	The Cancer Genome Atlas
TME	Tumor microenvironment
OS	Overall survival
PFS	Progression-free survival
DSS	Disease-specific survival
DFS	Disease-free survival
ACC	Adrenocortical Cancer
BLCA	Bladder Cancer
BRCA	Breast Cancer
CESC	Cervical Cancer
CHOL	Bile Duct Cancer
COAD	Colon Cancer

DLBC	Large B-cell Lymphoma
ESCA	Esophageal Cancer
GBM	Glioblastoma
HNSC	Head and Neck Cancer
KICH	Kidney Chromophobe
KIRC	Kidney Clear Cell Carcinoma
KIRP	Kidney Papillary Cell Carcinoma
LAML	Acute Myeloid Leukemia
LGG	Lower grade glioma
LIHC	Liver Cancer
LUAD	Lung Adenocarcinoma
LUSC	Lung Squamous Cell Carcinoma
MESO	Mesothelioma
OV	Ovarian Cancer
PAAD	Pancreatic Cancer
PCPG	Pheochromocytoma & Paraganglioma
PRAD	Prostate Cancer
READ	Rectal Cancer
SARC	Sarcoma
SKCM	Melanoma
STAD	Stomach Cancer
TGCT	Testicular Cancer
THCA	Thyroid Cancer
THYM	Thymoma
UCEC	Endometrioid Cancer
UCS	Uterine Carcinosarcoma
UVM	Uveal Melanoma
GSEA	Gene set enrichment analysis

Supplementary Information

The online version contains supplementary material available at https://doi.org/10.1186/s12885-025-14345-z.

Supplementary Material 1

Supplementary Material 2

Supplementary Material 3

Supplementary Material 4

Author contributions

MX and JZ drafted the article and interpreted data. MX and JL performed the experiments and obtained the data. YZ and JL designed the study.

Funding

This work was supported by the National Natural Science Foundation of China (grant numbers 81902612).

Data availability

The datasets supporting the conclusions of this article are included within the article and its additional files.

Declarations

Ethics approval and consent to participate

Informed consent was obtained from all patients. The use of these tissue samples was approved by the Ethics Committee of the First Affiliated Hospital of the Zhejiang University School of Medicine. All experiments were performed in accordance with relevant guidelines and regulations.

Consent for publication

Consent for publication was obtained from the participants.

Competing interests

The authors declare no competing interests.

Author details

[1]Department of Urology, First Affiliated Hospital, School of Medicine, Zhejiang University, Hangzhou, Zhejiang, China

[2]Department of Urology, Xiangshan Hospital of Wenzhou Medical University, Ningbo, Zhejiang, China

Received: 9 December 2024 / Accepted: 16 May 2025
Published online: 23 May 2025

References

1. Siegel RL, Miller KD, Wagle NS, Jemal A. Cancer statistics, 2023. Cancer J Clin. 2023;73(1):17–48.
2. Demicco M, Liu XZ, Leithner K, Fendt SM. Metabolic heterogeneity in cancer. Nat Metabolism. 2024;6(1):18–38.
3. Aden D, Sureka N, Zaheer S, Chaurasia JK, Zaheer S. Metabolic reprogramming in cancer: implications for immunosuppressive microenvironment. Immunology. 2024.
4. Serpa J. Metabolic remodeling as a way of adapting to tumor microenvironment (TME), a job of several holders. Adv Exp Med Biol. 2020;1219:1–34.
5. Mao Y, Xia Z, Xia W, Jiang P. Metabolic reprogramming, sensing, and cancer therapy. Cell Rep. 2024;43(12):115064.
6. Alfred Witjes J, Max Bruins H, Carrión A, Cathomas R, Compérat E, Efstathiou JA, et al. European association of urology guidelines on Muscle-invasive and metastatic bladder cancer: summary of the 2023 guidelines. Eur Urol. 2024;85(1):17–31.
7. Lopez-Beltran A, Cookson MS, Guercio BJ, Cheng L. Advances in diagnosis and treatment of bladder cancer. BMJ (Clinical Res ed). 2024;384:e076743.
8. Kang HW, Kim WJ, Choi W, Yun SJ. Tumor heterogeneity in muscle-invasive bladder cancer. Translational Androl Urol. 2020;9(6):2866–80.
9. Godlewski D, Bartusik-Aebisher D, Czech S, Szpara J, Aebisher D. Bladder cancer biomarkers. Explor Target anti-tumor Therapy. 2025;6:1002301.
10. Tran L, Xiao JF, Agarwal N, Duex JE, Theodorescu D. Advances in bladder cancer biology and therapy. Nat Rev Cancer. 2021;21(2):104–21.
11. Razavi S, Khan A, Fu DX, Mayer D, McConkey D, Putluri N, et al. Metabolic landscape in bladder cancer. Curr Opin Oncol. 2025;37(3):259–66.
12. Halestrap AP. The SLC16 gene family - structure, role and regulation in health and disease. Mol Aspects Med. 2013;34(2–3):337–49.
13. Felmlee MA, Jones RS, Rodriguez-Cruz V, Follman KE, Morris ME. Monocarboxylate transporters (SLC16): function, regulation, and role in health and disease. Pharmacol Rev. 2020;72(2):466–85.
14. Payen VL, Mina E, Van Hée VF, Porporato PE, Sonveaux P. Monocarboxylate transporters in cancer. Mol Metabolism. 2020;33:48–66.
15. Halestrap AP. The monocarboxylate transporter family–Structure and functional characterization. IUBMB Life. 2012;64(1):1–9.
16. Faubert B, Solmonson A, DeBerardinis RJ. Metabolic reprogramming and cancer progression. Volume 368. New York, NY: Science; 2020. 6487.
17. Vander Heiden MG, Cantley LC, Thompson CB. Understanding the Warburg effect: the metabolic requirements of cell proliferation. Sci (New York NY). 2009;324(5930):1029–33.
18. Bose S, Zhang C, Le A. Glucose metabolism in cancer: the warburg effect and beyond. Advances in experimental medicine and biology. 2021;1311:3–15.
19. Boedtkjer E, Pedersen SF. The acidic tumor microenvironment as a driver of Cancer. Annu Rev Physiol. 2020;82:103–26.
20. Singh M, Afonso J, Sharma D, Gupta R, Kumar V, Rani R et al. Targeting monocarboxylate transporters (MCTs) in cancer: how close are we to the clinics? Semin Cancer Biol. 2023;90:1–14.
21. Huang CK, Chang PH, Kuo WH, Chen CL, Jeng YM, Chang KJ, et al. Adipocytes promote malignant growth of breast tumours with monocarboxylate transporter 2 expression via β-hydroxybutyrate. Nat Commun. 2017;8:14706.
22. Chatterjee P, Bhowmik D, Roy SS. A systemic analysis of monocarboxylate transporters in ovarian cancer and possible therapeutic interventions. Channels (Austin Tex). 2023;17(1):2273008.
23. Valença I, Pértega-Gomes N, Vizcaino JR, Henrique RM, Lopes C, Baltazar F, et al. Localization of MCT2 at peroxisomes is associated with malignant transformation in prostate cancer. J Cell Mol Med. 2015;19(4):723–33.
24. Khalyfa A, Qiao Z, Raju M, Shyu CR, Coghill L, Ericsson A et al. Monocarboxylate Transporter-2 expression restricts tumor growth in a murine model of lung cancer: A Multi-Omic analysis. Int J Mol Sci. 2021;22(19).
25. Camacho M, Vázquez-López C, Valero C, Holgado A, Terra X, Avilés-Jurado FX, et al. Transcriptional expression of SLC16A7 as a biomarker of occult lymph node metastases in patients with head and neck squamous cell carcinoma. European archives of oto-rhino-laryngology: official journal of the European federation of Oto-Rhino-Laryngological societies (EUFOS): affiliated

with the German society for Oto-Rhino-Laryngology -. Head Neck Surg. 2024;281(12):6637–44.
26. Pinheiro C, Penna V, Morais-Santos F, Abrahão-Machado LF, Ribeiro G, Curcelli EC, et al. Characterization of monocarboxylate transporters (MCTs) expression in soft tissue sarcomas: distinct prognostic impact of MCT1 sub-cellular localization. J Translational Med. 2014;12:118.
27. Johnson JM, Cotzia P, Fratamico R, Mikkilineni L, Chen J, Colombo D, et al. MCT1 in invasive ductal carcinoma: monocarboxylate metabolism and aggressive breast Cancer. Front Cell Dev Biology. 2017;5:27.
28. Pinheiro C, Reis RM, Ricardo S, Longatto-Filho A, Schmitt F, Baltazar F. Expression of monocarboxylate transporters 1, 2, and 4 in human tumours and their association with CD147 and CD44. J Biomed Biotechnol. 2010;2010:427694.
29. Noble RA, Bell N, Blair H, Sikka A, Thomas H, Phillips N, et al. Inhibition of monocarboxyate transporter 1 by AZD3965 as a novel therapeutic approach for diffuse large B-cell lymphoma and Burkitt lymphoma. Haematologica. 2017;102(7):1247–57.
30. Sweeny L, Dean NR, Frederick JW, Magnuson JS, Carroll WR, Desmond RA, et al. CD147 expression in advanced cutaneous squamous cell carcinoma. J Cutan Pathol. 2012;39(6):603–9.
31. Simões-Sousa S, Granja S, Pinheiro C, Fernandes D, Longatto-Filho A, Laus AC, et al. Prognostic significance of monocarboxylate transporter expression in oral cavity tumors. Cell Cycle (Georgetown Tex). 2016;15(14):1865–73.
32. Wang C, Wen Z, Xie J, Zhao Y, Zhao L, Zhang S, et al. MACC1 mediates chemotherapy sensitivity of 5-FU and cisplatin via regulating MCT1 expression in gastric cancer. Biochem Biophys Res Commun. 2017;485(3):665–71.
33. Li Z, Wu Q, Sun S, Wu J, Li J, Zhang Y, et al. Monocarboxylate transporters in breast cancer and adipose tissue are novel biomarkers and potential therapeutic targets. Biochem Biophys Res Commun. 2018;501(4):962–7.
34. Dana P, Saisomboon S, Kariya R, Okada S, Obchoei S, Sawanyawisuth K, et al. CD147 augmented monocarboxylate transporter-1/4 expression through modulation of the Akt-FoxO3-NF-κB pathway promotes cholangiocarcinoma migration and invasion. Cell Oncol (Dordrecht Netherlands). 2020;43(2):211–22.
35. Pértega-Gomes N, Vizcaíno JR, Miranda-Gonçalves V, Pinheiro C, Silva J, Pereira H, et al. Monocarboxylate transporter 4 (MCT4) and CD147 overexpression is associated with poor prognosis in prostate cancer. BMC Cancer. 2011;11:312.
36. Liu Y, Sun X, Huo C, Sun C, Zhu J. Monocarboxylate transporter 4 (MCT4) overexpression is correlated with poor prognosis of osteosarcoma. Med Sci Monitor: Int Med J Experimental Clin Res. 2019;25:4278–84.
37. Huhta H, Helminen O, Palomäki S, Kauppila JH, Saarnio J, Lehenkari PP, et al. Intratumoral lactate metabolism in Barrett's esophagus and adenocarcinoma. Oncotarget. 2017;8(14):22894–902.
38. Zhu J, Wu YN, Zhang W, Zhang XM, Ding X, Li HQ, et al. Monocarboxylate transporter 4 facilitates cell proliferation and migration and is associated with poor prognosis in oral squamous cell carcinoma patients. PLoS ONE. 2014;9(1):e87904.
39. Chen HL, OuYang HY, Le Y, Jiang P, Tang H, Yu ZS, et al. Aberrant MCT4 and GLUT1 expression is correlated with early recurrence and poor prognosis of hepatocellular carcinoma after hepatectomy. Cancer Med. 2018;7(11):5339–50.
40. Alves VA, Pinheiro C, Morais-Santos F, Felipe-Silva A, Longatto-Filho A, Baltazar F. Characterization of monocarboxylate transporter activity in hepatocellular carcinoma. World J Gastroenterol. 2014;20(33):11780–7.
41. Sonveaux P, Végran F, Schroeder T, Wergin MC, Verrax J, Rabbani ZN, et al. Targeting lactate-fueled respiration selectively kills hypoxic tumor cells in mice. J Clin Investig. 2008;118(12):3930–42.
42. Payen VL, Brisson L, Dewhirst MW, Sonveaux P. Common responses of tumors and wounds to hypoxia. Cancer J (Sudbury Mass). 2015;21(2):75–87.
43. Végran F, Boidot R, Michiels C, Sonveaux P, Feron O. Lactate influx through the endothelial cell monocarboxylate transporter MCT1 supports an NF-κB/IL-8 pathway that drives tumor angiogenesis. Cancer Res. 2011;71(7):2550–60.
44. Sonveaux P, Copetti T, De Saedeleer CJ, Végran F, Verrax J, Kennedy KM, et al. Targeting the lactate transporter MCT1 in endothelial cells inhibits lactate-induced HIF-1 activation and tumor angiogenesis. PLoS ONE. 2012;7(3):e33418.
45. De Saedeleer CJ, Copetti T, Porporato PE, Verrax J, Feron O, Sonveaux P. Lactate activates HIF-1 in oxidative but not in Warburg-phenotype human tumor cells. PLoS ONE. 2012;7(10):e46571.
46. Fallah A, Sadeghinia A, Kahroba H, Samadi A, Heidari HR, Bradaran B, et al. Therapeutic targeting of angiogenesis molecular pathways in angiogenesis-dependent diseases. Biomed pharmacotherapy = Biomedecine Pharmacotherapie. 2019;110:775–85.
47. Kumar A, Sunita P, Jha S, Pattanayak SP. Daphnetin inhibits TNF-α and VEGF-induced angiogenesis through Inhibition of the IKKs/IκBα/NF-κB, Src/FAK/ERK1/2 and Akt signalling pathways. Clin Exp Pharmacol Physiol. 2016;43(10):939–50.
48. Wang L, Niu Z, Wang X, Li Z, Liu Y, Luo F, et al. PHD2 exerts anti-cancer and anti-inflammatory effects in colon cancer xenografts mice via attenuating NF-κB activity. Life Sci. 2020;242:117167.
49. Curtis NJ, Mooney L, Hopcroft L, Michopoulos F, Whalley N, Zhong H, et al. Pre-clinical Pharmacology of AZD3965, a selective inhibitor of MCT1: DLBCL, NHL and Burkitt's lymphoma anti-tumor activity. Oncotarget. 2017;8(41):69219–36.
50. Guan X, Rodriguez-Cruz V, Morris ME. Cellular uptake of MCT1 inhibitors AR-C155858 and AZD3965 and their effects on MCT-Mediated transport of L-Lactate in murine 4T1 breast tumor Cancer cells. AAPS J. 2019;21(2):13.
51. Brand A, Singer K, Koehl GE, Kolitzus M, Schoenhammer G, Thiel A, et al. LDHA-Associated lactic acid production blunts tumor immunosurveillance by T and NK cells. Cell Metabol. 2016;24(5):657–71.
52. Yu T, Liu Z, Tao Q, Xu X, Li X, Li Y, et al. Targeting tumor-intrinsic SLC16A3 to enhance anti-PD-1 efficacy via tumor immune microenvironment reprogramming. Cancer Lett. 2024;589:216824.

Publisher's note